Experimental analysis of valence-band photoemission intensities for Cu(111) and Cu(100)

A. Gerlach, R. Matzdorf, and A. Goldmann
Fachbereich Physik, Universität Kassel, Heinrich-Plett-Strasse 40, D-34132 Kassel, Germany
(Received 12 May 1998)

Angle-resolved photoemission with *p*-polarized He I radiation has been used to study transition matrix elements of bulk direct transitions in copper. From peak intensities as a function of light incidence angle the direction and relative magnitude of the momentum matrix element $\mathbf{P}_{\mathrm{fi}}=\langle f|\mathbf{p}|i\rangle$ have been determined. At a fixed point in *k* space $\mathbf{P}_{\mathrm{fi}}$ is independent of the special experimental geometry and depends only on the initial- and final-state wave function. Therefore it is particularly suitable for comparison to theory. We present measurements of the momentum matrix element for bulk transitions out of *d*- and *sp*-like bands. Selected *k*-space points have been triangulated from Cu(111) and Cu(100) surfaces. Within the error bars direction and absolute value of $\mathbf{P}_{\mathrm{fi}}$ are found to be independent of the particular surface. This shows that the description of the matrix element in terms of bulk direct interband transitions may be a reasonable approximation in many cases. Moreover these results demonstrate that the macroscopic Fresnel equations are appropriate to describe the light properties inside the sample under the experimental conditions of our experiment. [S0163-1829(98)07240-3]

I. INTRODUCTION

In the past two decades angle-resolved photoemission has been used very successfully to measure solid state properties with resolution in the reciprocal space. In particular the binding energy of the electrons as a function of the wave vector $E_i(\mathbf{k})$, i.e., the band structure has been studied.[1–3] In addition, the lifetime of the initial state $|i\rangle$ and the final state $|f\rangle$ involved in the photoemission process can be measured in favorable cases by linewidth analysis.[1–7] As a third quantity the squared photoemission matrix element may be extracted from experiment by analysis of line intensities. This quantity, although very interesting for comparison to theoretical calculations, has been studied less than the others. Matrix elements are more sensitive to the involved wave functions than the energy eigenvalues and can be used to examine the wave functions from *ab initio* band-structure calculations.

However, the transition matrix element contains the vector potential of the photon field and therefore it depends strongly on the polarization and incidence angle of the UV light. For comparison to theory it is thus very helpful to separate the light properties from the crystal properties. This can be done by splitting the matrix element of the dipole operator in a product of the vector potential and a ''momentum matrix element'' $\mathbf{P}_{\mathrm{fi}}$, which depends only on the initial- and final-state wave functions.[8–13] The quantity $\mathbf{P}_{\mathrm{fi}}$ (for details see below) may be investigated by measurements dependent on light incidence and light polarization angles, as suggested already very early[8] and attempted experimentally later.[9–13] Earlier studies of matrix element effects and photoemission intensities calculated electron energy distribution curves based on either the three-step model of photoemission (see, e.g., Refs. 10, 11, 14–16) or on calculations using the one-step model.[17,18] However, a really satisfying agreement with experimental spectra was not obtained. In three-step-model calculations the component of the vector potential perpendicular to the surface (as calculated using the macroscopic optical constants) have to be suppressed by an order of magnitude (as compared to the components parallel to the surface) in order to obtain spectra that reflect the experimental results.[11] The one-step-model calculations do not require an artificial suppression of the vector potential normal to the surface, and they sometimes are able (after an empirical adjustment of the potential in the outermost layer of the sample, see Ref. 17) to reproduce experimental spectra comparatively well. However, in other cases the overall agreement is not convincing at all.[18]

We attempt to study photoemission intensities. Our hope to gain insight relies on a better experimental resolution than applied in the earlier studies, and, in particular, a larger database of spectra collected at a much wider range of photon incidence angles than used before. In fact the momentum matrix element is in general a complex vector and the experimental determination of its components requires many spectra. We have chosen copper as a ''standard test material'' of photoemission. Its surfaces may be prepared sufficiently well and its electronic properties are understood[3,14] in considerable detail.

II. THEORETICAL CONSIDERATIONS

The interaction Hamiltonian in photoemission can be written[1–3] in the nonrelativistic limit after neglecting a term in $\mathbf{A}^2$:

$$H_{\mathrm{int}}=\frac{e}{2mc}\left(2\mathbf{A}\cdot\mathbf{p}+\frac{\hbar}{i}\,\mathrm{div}\,\mathbf{A}\right) \tag{1}$$

with the vector potential $\mathbf{A}$ and the momentum operator $\mathbf{p}$. The first term is responsible for direct transitions,[1–3] the other one results in surface emission.[19–23] In time-dependent perturbation theory the transition rate from initial state $|i\rangle$ to final state $|f\rangle$ is expressed by Fermi's ''golden rule''

$$w\propto\frac{2\pi}{\hbar}\,|M_{fi}|^2\,\delta(E_f-E_i-\hbar\omega)\,\rho(E_f) \tag{2}$$

with the initial- and final-state energies E_i and E_f, the photon energy $\hbar\omega$, the density of final states $\rho(E_f)$ and the matrix element

$$M_{fi}=\frac{e}{mc}\langle f|\mathbf{A}\cdot\mathbf{p}|i\rangle+\frac{e\hbar}{i2mc}\langle f|\text{div }\mathbf{A}|i\rangle. \tag{3}$$

In our following consideration we will neglect surface emission, but come back to it in the conclusions. Furthermore, we neglect the space dependence of $\mathbf{A}$ since the wavelength of the UV light is large compared to atomic distances. This ''dipole'' approximation allows one to rewrite the matrix element as a scalar product:

$$M_{fi}=\frac{e}{mc}\,\mathbf{A}\cdot\langle f|\mathbf{p}|i\rangle=\frac{e}{mc}\,\mathbf{A}\cdot\mathbf{P}_{\text{fi}} \tag{4}$$

with the momentum matrix element $\mathbf{P}_{\text{fi}}$.

The final state $|f\rangle$ is not a superposition of all degenerate states with energy E_f, as generally considered in the derivation of Fermi's ''golden rule.'' Due to the angle-resolved detection of the electron in vacuum the final state is a linear combination of those states with energy E_f that couple to the plane wave in vacuum, a so-called inverted LEED state.[24,25] We must be aware of the fact that in this sense $\mathbf{P}_{\text{fi}}$ is a special momentum matrix element which describes a transition into the detected photoemission final state. As a consequence $\mathbf{P}_{\text{fi}}$ is a complex vector in general. The aim of our experiments is to determine the relative size of its real and imaginary parts.

In the relativistic formalism the interaction Hamiltonian is given by[29]

$$H_{\text{int}}=e\,\boldsymbol{\alpha}\cdot\mathbf{A}. \tag{5}$$

[In Eqs. (5)–(7) we use Coulomb gauge and $m=\hbar=c=1$.] Within the dipole approximation and using Fermi's ''golden rule'' formula the matrix element reads

$$M_{fi}=e\langle f|\,\boldsymbol{\alpha}\cdot\mathbf{A}|i\rangle. \tag{6}$$

After some further approximations similar to the nonrelativistic case this can be written in close analogy to Eq. (4) as

$$M_{fi}=e\mathbf{A}\cdot\langle f|\,\boldsymbol{\alpha}|i\rangle=e\mathbf{A}\cdot\mathbf{P}_{\text{fi}}. \tag{7}$$

The three components of the vector $\boldsymbol{\alpha}$ are the (4×4) Dirac matrices and $|f\rangle$ and $|i\rangle$ are spinors with 4 components. As a consequence, the three components of the vector $\mathbf{P}_{\text{fi}}$ are complex numbers in the relativistic case as well.

The photoemission process is governed by the transmitted vector potential $\mathbf{A}^t$ in the outermost few Å of the solid. Up to now it is a matter of debate[9–25] to which extent $\mathbf{A}^t$ may be described correctly by the Fresnel equations,[26] which are valid on a length scale given by the attenuation length of the UV light (113 Å in copper at $\hbar\omega=21.2$ eV). Nevertheless, in the following we will use the Fresnel equations for our data analysis. Since all our experimental data are fully consistent with this formulation, we conclude that for our experiments the use of the Fresnel equations is justified.

Since the UV light is partially absorbed by the metal surface, the index of refraction becomes complex $n=\sqrt{\epsilon}=\sqrt{\epsilon_1+i\epsilon_2}$, where ϵ_1 and ϵ_2 are the real and imaginary parts of the dielectric function. The law of refraction remains valid[26]

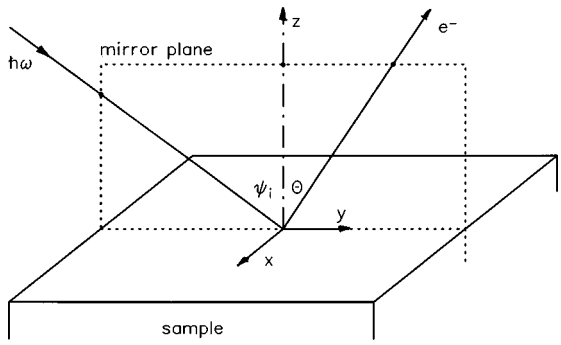

FIG. 1. Geometry of experiments in a mirror plane of the bulk lattice. The light polarization angle α_i is defined such that $\alpha_i=90°$ when the vector potential is oriented along the x direction.

$$\sin\,\psi_t=\frac{1}{n}\sin\,\psi_i \tag{8}$$

with incidence angle ψ_i and the complex transmission angle ψ_t. The Fresnel equations read

$$A_{\parallel}^t=\frac{2\cos\,\psi_i}{n\cos\,\psi_i+\cos\,\psi_t}\,A_{\parallel}^i, \tag{9}$$

$$A_{\perp}^t=\frac{2\cos\,\psi_i}{\cos\,\psi_i+n\cos\,\psi_t}\,A_{\perp}^i \tag{10}$$

with the components of the vector potential parallel $A_{\parallel}$ and perpendicular $A_{\perp}$ to the plane of incidence. The three Cartesian components of $\mathbf{A}^t$ are deduced to be[27]

$$A_x^t=\frac{2\cos\,\psi_i\sin\,\alpha_i}{\cos\,\psi_i+\sqrt{\epsilon-\sin^2\psi_i}}\,|\mathbf{A}_i|, \tag{11}$$

$$A_y^t=\frac{2\sqrt{\epsilon-\sin^2\psi_i}\,\cos\,\psi_i\cos\,\alpha_i}{\epsilon\cos\,\psi_i+\sqrt{\epsilon-\sin^2\psi_i}}\,|\mathbf{A}_i|, \tag{12}$$

$$A_z^t=\frac{2\cos\,\psi_i\sin\,\psi_i\cos\,\alpha_i}{\epsilon\cos\,\psi_i+\sqrt{\epsilon-\sin^2\psi_i}}\,|\mathbf{A}_i|, \tag{13}$$

where z is the surface normal direction, yz is the plane of incidence, and α_i is the polarization angle ($\alpha_i=0°$: p polarization; $\alpha_i=90°$: s polarization). The components of $\mathbf{A}^t$ are complex due to phase shifts between them.

In the Cartesian coordinates the transition matrix element is given by

$$M_{fi}=A_x^tP_x^*+A_y^tP_y^*+A_z^tP_z^* \tag{14}$$

with the conjugate complex components P_x^*, P_y^*, and P_z^* of the vector $\mathbf{P}_{\text{fi}}$. Since only $|M_{fi}|^2$ is an observable, one phase factor in the matrix element is undefined and we can choose, for example, P_z to be real.

For simplification we have used in our experiments a geometry where the plane of light incidence, surface normal direction, and electron emission direction coincide with a mirror plane of the bulk lattice (Fig. 1). In this geometry and in the nonrelativistic limit the wave functions are odd or even with respect to the mirror plane and, as a consequence, the vector $\mathbf{P}_{\text{fi}}$ is oriented either in plane ($P_x=0$) or perpen-

dicular to it ($P_y = P_z = 0$). For a measurement of an in-plane vector exclusively *p*-polarized light may be used and *s*-polarized light for a vector perpendicular to the plane.

In the relativistic case the spin orbit interaction intermixes even and odd states, which may result in a $\mathbf{P}_{\mathrm{fi}}$ that has all vector components $\neq 0$. Due to mirror symmetry the experimental intensity remains unchanged if α_i is replaced by $-\alpha_i$. Using Eqs. (11)–(13) this results in the identity

$$|A_x^t P_x^* + A_y^t P_y^* + A_z^t P_z^*|^2 = |-A_x^t P_x^* + A_y^t P_y^* + A_z^t P_z^*|^2 \tag{15}$$

even in the presence of spin-orbit coupling. As a consequence, the intensity can be written as an incoherent superposition of intensities excited with 100% *s*-polarized and 100% *p*-polarized light, respectively:

$$I \propto |A_x^t P_x^*|^2 + |A_y^t P_y^* + A_z^t P_z^*|^2. \tag{16}$$

We have verified this experimentally by analyzing spectra taken for many polarization angles α_i keeping the light incidence angle ψ_i constant.

In all other experiments we have used exclusively *p*-polarized light to determine the vector components P_y and P_z. For this purpose we have varied the light incidence angle ψ_i resulting in a rotation of $\mathbf{A}^t$ with respect to $\mathbf{P}_{\mathrm{fi}}$. The intensity as a function of ψ_i is given by

$$I(\psi_i) \propto |A_y^t(\psi_i) P_y^* + A_z^t(\psi_i) P_z^*|^2. \tag{17}$$

From the best fit to the measured dependence $I(\psi_i)$ we have determined P_y and P_z, which was chosen to be real. For the actual fit of the experimental data other parameters are mathematically better adapted: We can express the components of the momentum matrix element

$$P_z = \|\mathbf{P}_{\mathrm{fi}}\| \cos\beta, \tag{18}$$

$$P_y = \|\mathbf{P}_{\mathrm{fi}}\| \sin\beta e^{i\gamma}, \tag{19}$$

with $\|\mathbf{P}_{\mathrm{fi}}\| = \sqrt{|P_y|^2 + |P_z|^2}$. β is the angle between $(|P_y|, P_z)$ and the surface normal direction, γ is a phase angle representing a phase shift between P_z and P_y. The absolute value of $\mathbf{P}_{\mathrm{fi}}$ cannot be measured very reliably, since the absolute intensity in a photoemission experiment depends on many experimental parameters. In contrast, relative changes of $\|\mathbf{P}_{\mathrm{fi}}\|$ as a function of wave vector $\mathbf{k}$ as well as a comparison of emission out of different bulk bands within one spectrum is easily possible. However, both angles can be determined absolutely from the shape of the function $I(\psi_i)$. Therefore β and γ are most reliable and relevant for a comparison of experimental and theoretical results.

This experimental determination of $\mathbf{P}_{\mathrm{fi}}$ is purely empirical: Observed photoemission intensities contain the full information about the involved wave functions. For example, it should be possible to identify any changes in the character of the final state as the wave vector crosses the zone boundary, giving rise to a variation of the corresponding matrix elements $\mathbf{P}_{\mathrm{fi}}$. The concomitant appearance or disappearance of emission has often been used to identify $k_\perp$ components in band-structure investigations (''Bragg plane method''[3]).

III. EXPERIMENTAL DETAILS

The single-crystal copper samples have been polished mechanically and electrochemically, cleaned *in situ* by argon ion bombardment and subsequent annealing. During measurements the sample has been cooled by liquid nitrogen to $T = 170$ K to reduce line broadening by electron-phonon and/or hole-phonon interactions. The azimuthal orientation of the crystal has been adjusted by using a LEED system. The electron energy analyzer is operated at an energy resolution of $\Delta E = 25$ meV and an angular resolution of $\Delta\theta = \pm 1.5°$. It is equipped with a modified lens system that allows one to collect electrons from an extended area (6 mm×6 mm) on the sample without loss of energy or angular resolution. The *p*-polarized light has been produced by a self-built capillary discharge lamp equipped with an arrangement of three gold-coated mirrors. The polarizer can be turned around the sample, allowing light incidence angles ψ_i between $-90°$ and $+90°$. The UV light is focused onto the sample in a way that even at grazing incidence angles up to $\psi = \pm 85°$ the light spot on the sample is elongated less than 6 mm. The degree of polarization is $93 \pm 1\%$ and the angular spread of the incident light due to focusing is $\pm 5°$. Due to the well tuned electron lens and polarizer there is no loss in intensity by geometrical effects when ψ_i is changed. Unfortunately, there is an angular range of $\pm 30°$ around the electron emission direction that is not yet accessible as light incidence direction. We will change our construction to close this gap for future work. The lens system and the polarizer have been described in more detail elsewhere.[28]

IV. RESULTS

We have collected a very large number of spectra for different electron emission angles θ and light incidence angles ψ_i on Cu(111) and Cu(100). For presentation of typical results we show in Fig. 2 spectra measured on Cu(111) in the ΓLUX mirror plane at fixed angle $\theta = 40°$ and different ψ_i. The peaks labeled $A-E$ are direct transitions between the bulk bands of copper, which have been well known for many years.[14] We can clearly see that peak intensities change considerably from one spectrum to another. Since the peaks $B-E$ are strongly overlapping, a fit procedure is required to determine peak intensities reliably. An assumption of simple peak shapes like Gaussian or Lorentzians for a fit is not adequate since the peak shapes are strongly dependent on the band dispersions.[6,7] Therefore we have used a procedure that calculates the line shape of every peak separately. It includes both the energy dispersion of the initial- and final-state bands (which is taken from the well-known band structure of copper) and the energy-dependent lifetime width of photohole and excited electron. The calculational procedure is described in great detail in Sec. III of Ref. 7 and will not be repeated here. These calculated peak shapes have been used to fit the whole spectrum together with a background given by a polynomial of second order. From this fit the peak intensities (areas) have been taken and plotted (filled circles) as a function of light incidence angle in Fig. 3. These data are collected from a series of about 20 spectra taken for $-85° < \psi_i < -75°$ and $-5° < \psi_i < 85°$. The angular range between $-75°$ and $-5°$ is not accessible in our experimental

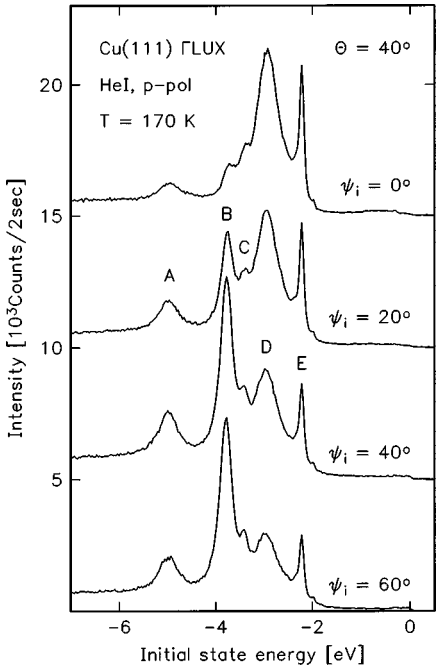

FIG. 2. Electron energy distribution curves taken with 93% *p*-polarized He I radiation. Spectra are shown for different light incidence angles ψ_i at fixed electron emission angle $\theta = 40°$. The peaks are labeled from left to the right by $A-E$. Intensities are plotted as measured, the spectra are shifted against each other by 5 units of the ordinate scale.

setup. We have fitted the data with a function given by Eq. (17) using the components of the vector potential $\mathbf{A}^t$ according to Eqs. (12) and (13). The components of $\mathbf{P}_{\rm fi}$ are then obtained by adjusting the parameters $\|\mathbf{P}_{\rm fi}\|$, β, and γ according to Eqs. (18) and (19). The results are collected in Table I.

From Fig. 3 we clearly see that experimental data can be fitted very well by this procedure. All other data we have collected on Cu(100) and Cu(111) at different (θ, ψ_i) combinations can be fitted with similar quality. We conclude that our formalism—based on the macroscopic Fresnel equations—is sufficiently convenient and accurate for a determination of the photoemission matrix element in our experiments. We have used the dielectric function $\epsilon(21.2\ \text{eV}) = 0.63 + i0.74$ determined by reflectivity measurements.[30]

TABLE I. Parameters used for the fits (solid lines) in Figs. 3 and 4. From these parameters the components of the momentum matrix element $\mathbf{P}_{\rm fi}$ are calculated with Eqs. (16) and (17).

Θ (deg)	Peak	β (deg)	γ (deg)	$\|\mathbf{P}_{\rm fi}\|$ (a.u.)
40	*A*	31	−12	29
40	*B*	16	−20	55
40	*D*	68	142	48
40	*E*	60	140	21
10	$E_i = -3.86$ eV	10	86	53
10	$E_i = -3.50$ eV	20	−56	29
45	$E_i = -0.48$ eV	29	178	21
60	$E_i = -1.53$ eV	10	−130	33

In Fig. 4 we reproduce additional examples of $I(\psi_i)$ curves. We would like to emphasize that measurements restricted to $\psi_i > 0$ are generally not sufficient for a reliable determination of $\mathbf{P}_{\rm fi}$. This experimental restriction, however, was present in previous publications dealing with the problem.[12,13] Even in our experimental setup the inaccessible gap of 60° may result in large errors in the determination of β and especially of γ. From our experience in fitting we can say that intensities $I(\psi_i)$ like the ones in Fig. 4 give an excellent agreement if both maxima and the minimum are represented by data points. The fit is less reliable if one maximum or minimum is not observed. The angles β and γ are especially sensitive to the relative height and the position of the maxima as well as to position and depth of the minimum. If functions are to be fitted of the type as shown in Fig. 3 in the two lower panels, the position of the maximum and the shape around the maximum are of special interest. The error of β in our fits is rather small and in most cases less than $\pm 5°$. In contrast, γ can be determined less reliably. This

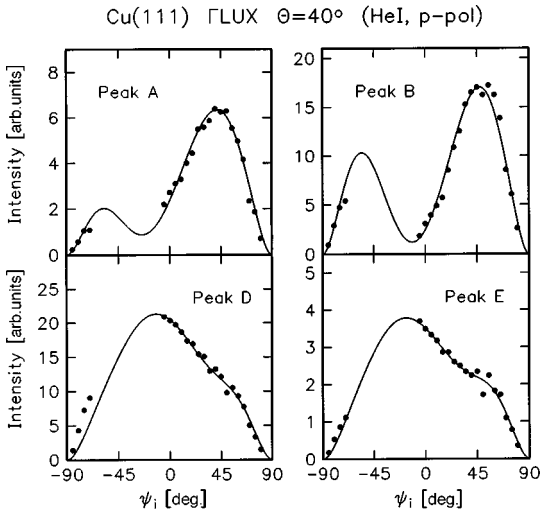

FIG. 3. Peak intensities of peaks *A*, *B*, *D*, and *E* in Fig. 2 as a function of light incidence angle ψ_i. Filled circles: Intensity as extracted from measured spectra. Solid line: Best fit to the data used for determination of $\mathbf{P}_{\rm fi}$.

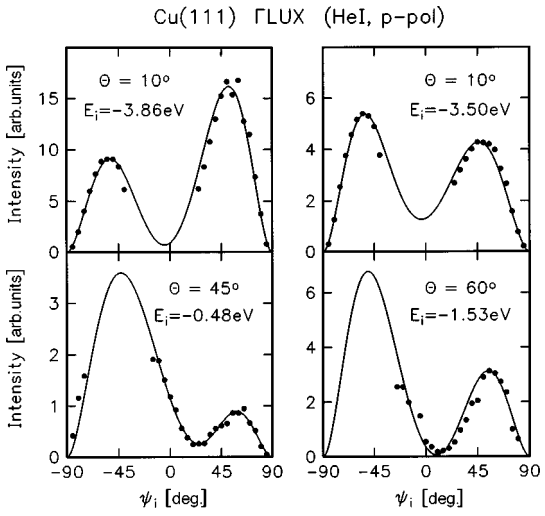

FIG. 4. Other examples of peak intensities *I* as a function of light incidence angle ψ_i. Filled circles: Intensity as extracted from measured spectra. Solid line: Best fit to the data used for determination of $\mathbf{P}_{\rm fi}$.

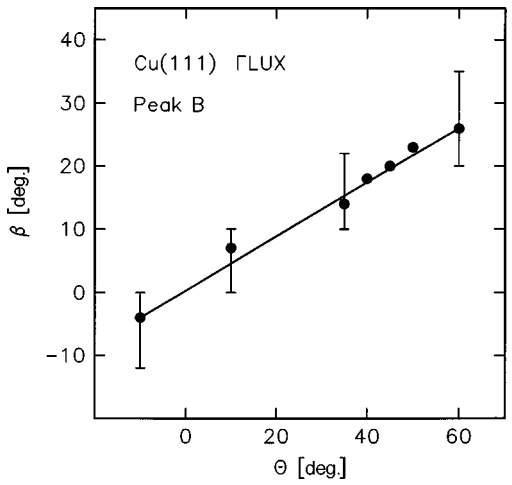

FIG. 5. Direction β of the momentum matrix element $\mathbf{P}_{\mathrm{fi}}$ with respect to the surface normal as function of electron emission angle θ in the ΓLUX plane of Cu(111) for transitions out of the lowest *d*-like states (compare peak *B* in Fig. 2). The data are obtained from an analysis as shown in Figs. 3 and 4. Filled circles: experimental data, solid line: linear fit.

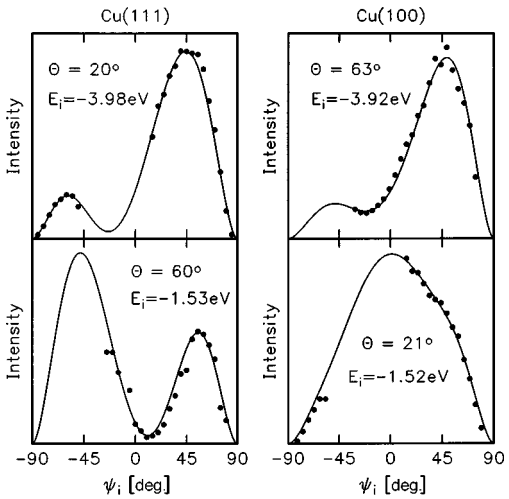

FIG. 6. Peak intensities as a function of light incidence angle ψ_i. Triangulated transitions from Cu(111) (left column) and Cu(100) (right column). Filled circles: Intensity as extracted from measured spectra. Solid line: Best fit to the data used for determination of $\mathbf{P}_{\mathrm{fi}}$.

results from the fact that for $\beta=0°$ ($P_y=0$) and $\beta=90°$ ($P_z=0$) γ is completely undefined. For angles around these extremal cases γ is sensitively dependent on small changes in $I(\psi_i)$ and therefore will have a large experimental error. Fit results obtained for the $I(\psi_i)$ data of Fig. 4 are collected in the lower panel of Table I.

In a further step we can investigate how the quantities $\|\mathbf{P}_{fi}\|$, β, and γ depend on the wave vector $\mathbf{k}$. As an example, we have picked out a move through *k* space by changing the electron emission angle θ in the ΓLUX plane of Cu(111) and have extracted the angle β, which can be determined reliably. In Fig. 5 the dependence $\beta(\theta)$ is shown for transitions out of *d*-like states corresponding to peak *B* at $\theta=40°$ in Fig. 2. We observe an essentially linear dependence with a slope of about 0.43. $\mathbf{P}_{\mathrm{fi}}$ is oriented along the surface normal direction at $\theta=0°$ and it turns to $\beta=26°$ with respect to the surface normal for electron emission at $\theta=60°$.

As mentioned in the Introduction the momentum matrix element depends only on the initial- and final-state wave functions. If they are not influenced by the surface, $\mathbf{P}_{\mathrm{fi}}$ depends only on $\mathbf{k}$ and on the used photon energy. To check for this we have investigated $\mathbf{P}_{\mathrm{fi}}$ for direct transitions occurring at the same point of the three-dimensional *k* space by observing them from differently oriented surfaces (''triangulation'' using the energy coincidence method[3]). Figure 6 shows the corresponding $I(\psi_i)$ results. For example a particular *d*-band emission occurring at $E_i=-3.98$ eV is observed at $\theta=20°$ on Cu(111). The same direct transition is registered at $\theta=63°$ on Cu(100). Similar data were collected for a direct *sp*-band transition registered at $E_i=-1.53$ eV and emitting at $\theta=60°$ and $\theta=21°$ on Cu(111) and Cu(100), respectively. The intensities in the lower panels of Fig. 6 are fitted with the angles $\beta_{\mathrm{Cu(111)}}=14\pm2°$ and $\beta_{\mathrm{Cu(100)}}=74\pm4°$. Both angles are measured with respect to the surface normal direction. For a comparison we take β' with respect to the bulk lattice [100] direction and find $\beta'_{\mathrm{Cu(111)}}=68.7\pm2°$ and $\beta_{\mathrm{Cu(100)}}=\beta=74\pm4°$, which agree within the experimental error. The intensities in the upper panels are fitted with $\beta_{\mathrm{Cu(111)}}=26\pm6°$ and $\beta_{\mathrm{Cu(100)}}=-26\pm3°$. This results in $\beta_{\mathrm{Cu(111)}}=-28.7\pm6°$ and $\beta'_{\mathrm{Cu(100)}}=-26\pm3°$, which agree as well. These both peaks have been triangulated very reliably by initial-state energy coincidence. Other examples of triangulated peaks show larger experimental errors in the determination of β either due to a less reliable triangulation (because of slow dispersion of peak positions with emission angle θ) or due to larger errors in the determination of β from the measured dependence $I(\psi_i)$. From our data set we cannot conclude that β' agrees in general.

There are indeed several arguments to expect disagreement of $\mathbf{P}_{fi}$ in a triangulation experiment. First, the superposition of final-state Bloch functions that couple to the plane wave in vacuum may be different if emission from different surfaces is investigated. Second, due to the finite lifetime of the final state its wave function is damped perpendicular to the surface. This damping may be different for different surfaces. As a consequence $\mathbf{P}_{\mathrm{fi}}$ is no pure bulk property. And third, intensity modifications during transmission of the electron through the surface (surface Umklapp processes, etc.) may be relevant. In all these cases the final-state wave function is altered. On the other hand, the initial state can be influenced by the presence of the surface (surface resonances). As another effect surface emission may be relevant resulting in a change of the measured intensities due to interference with bulk direct transitions [Eq. (3) and Refs. 19–23].

V. CONCLUSIONS

We have demonstrated that photoemission intensities in bulk direct transitions for Cu(111) and Cu(100) exited with $\hbar\omega=21.2$ eV are well described by $I\propto|\mathbf{A}\cdot\langle f|\mathbf{p}|i\rangle|^2$ with the vector potential calculated from Fresnel's equations and the complex momentum matrix element. Its components can be determined from measured intensities as a function of light incidence and polarization angle. Especially the direction of $\langle f|\mathbf{p}|i\rangle$ can be measured reliably. It is particularly suitable

for comparison to theory and can be used to verify the quality of wave functions. We will present a comparison of our experimental data with one-step calculations in a subsequent paper. Furthermore we have triangulated the momentum matrix element from different copper surfaces, which is interesting since the final-state wave function may be different on these surfaces. In selected examples we have found that the direction of $\langle f|\mathbf{p}|i\rangle$ is independent from the surface on which it has been measured. These experiments are additionally interesting with respect to the question of surface emission since they offer the possibility to distinguish between bulk emission and modifications induced by surface effects.

ACKNOWLEDGMENTS

We gratefully acknowledge continuous support from the Deutsche Forschungsgemeinschaft. We thank G. Meister for stimulating discussions.

[1] *Photoemission and the Electronic Properties of Surfaces*, edited by B. Feuerbacher, B. Fitton, and R. F. Willis (Wiley, New York, 1978).
[2] *Angle-Resolved Photoemission*, edited by S. D. Kevan, Studies in Surface Science and Catalysis Vol. 74 (Elsevier, Amsterdam, 1992).
[3] S. Hüfner, *Photoelectron Spectroscopy—Principles and Applications*, Springer Series in Solid-State Science Vol. 82 (Springer, Berlin, 1995).
[4] N. V. Smith, Comments Condens. Matter Phys. **15**, 263 (1992).
[5] N. V. Smith, P. Thiry, and Y. Petroff, Phys. Rev. B **47**, 15 476 (1993).
[6] R. Matzdorf, Appl. Phys. A: Mater. Sci. Process. **63**, 549 (1996).
[7] R. Matzdorf, Surf. Sci. Rep. **30**, 153 (1998).
[8] P. J. Feibelman, Surf. Sci. **46**, 558 (1974).
[9] S. P. Weeks and E. W. Plummer, Solid State Commun. **21**, 695 (1977).
[10] N. V. Smith, Phys. Rev. B **19**, 5019 (1979).
[11] N. V. Smith, R. L. Benbow, and Z. Hurych, Phys. Rev. B **21**, 4331 (1980).
[12] H. Wern and R. Courths, Surf. Sci. **152/153**, 196 (1985).
[13] H. Wern, R. Courths, Surf. Sci. **162**, 29 (1985).
[14] R. Courths and S. Hüfner, Phys. Rep. **112**, 53 (1984), and references therein to earlier work.
[15] H. Przybylski, A. Baalmann, G. Borstel, and M. Neumann, Phys. Rev. B **27**, 6669 (1983); G. Borstel, H. Przybylski, M. Neumann, and M. Wöhlecke, *ibid.* **25**, 2006 (1982).
[16] S. Holloway, D. E. Grider, and J. K. Sass, Solid State Commun. **39**, 953 (1981).
[17] P. O. Nilsson, J. Kanski, and C. G. Larsson, Solid State Commun. **36**, 111 (1980).
[18] A. Goldmann, A. Rodriguez, and R. Feder, Solid State Commun. **45**, 449 (1983).
[19] H. J. Levinson, E. W. Plummer, and P. J. Feibelman, Phys. Rev. Lett. **43**, 952 (1979).
[20] T. Miller, W. E. McMahon, and T.-C. Chiang, Phys. Rev. Lett. **77**, 1167 (1996).
[21] T. Miller, E. D. Hansen, W. E. McMahon, and T.-C. Chiang, Surf. Sci. **376**, 32 (1997).
[22] E. D. Hansen, T. Miller, and T.-C. Chiang, Phys. Rev. B **55**, 1871 (1997).
[23] E. D. Hansen, T. Miller, and T.-C. Chiang, Phys. Rev. Lett. **78**, 2807 (1997).
[24] J. B. Pendry, *Low Energy Electron Diffraction* (Academic Press, London, 1974).
[25] J. E. Inglesfield and E. W. Plummer, in *Angle-Resolved Photoemission* (Ref. 2), Chap. 2.
[26] M. Born and E. Wolf, *Principles of Optics* (Pergamon Press, Oxford, 1970).
[27] M. A. B. Whitaker, J. Phys. C **11**, L151 (1978).
[28] R. Matzdorf, A. Gerlach, R. Hennig, G. Lauff, and A. Goldmann, J. Electron. Spectrosc. Relat. Phenom. **94**, 279 (1998).
[29] G. Thörner and G. Borstel, Phys. Status Solidi B **126**, 617 (1984).
[30] H. J. Hagemann, W. Gudat, and C. Kunz, J. Opt. Soc. Am. **65**, 742 (1975).